

Recent results from LIGO and Virgo searches of continuous gravitational waves



Cristiano Palomba (INFN Roma)
on behalf of the LIGO/Virgo/Kagra Collaborations



Talk outline

- Sources of continuous gravitational waves (CWs)
- Searches for CWs
- Some recent search results
- Future prospects

DCC G2101170

Sources of Gravitational Waves (GW)

Transient

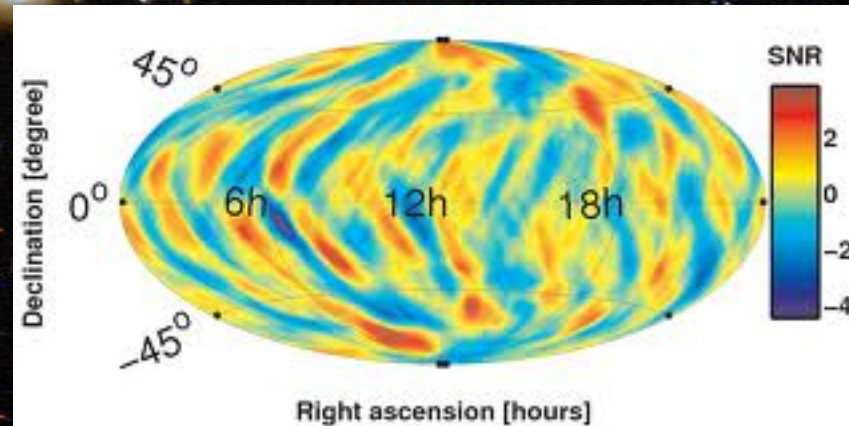
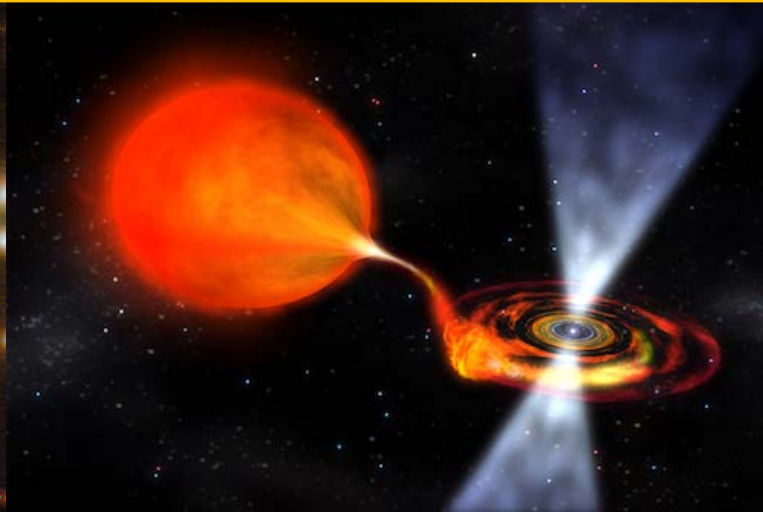
Modeled



Un-modeled



Persistent



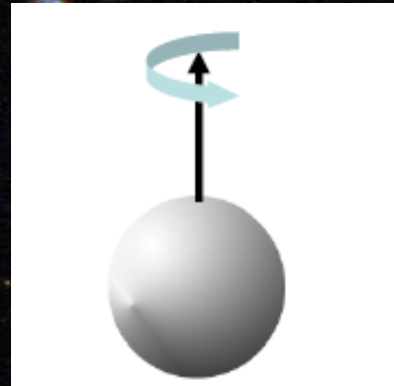
CW signals

Persistent, semi-periodic signals, with duration much larger than the typical observation times (months-years)

CW are emitted by spinning neutron stars, if asymmetric with respect to their rotation axis: constant amplitude, small spin-down

Asymmetry can be due to:

- elastic stresses in the star body
- inner magnetic field not aligned to the rotation axis
- matter accretion from a companion star
- excitation of long-lasting oscillations (like r-modes).
-



○ **We KNOW that potential sources of CW exist:** more than 3,000 NS are observed through their EM emission, up to 1 billion are expected to exist in the Galaxy

○ **We DO NOT KNOW the amplitude of the emitted signals**

$$h_0 \cong 10^{-27} \left(\frac{I_{zz}}{10^{38} \text{ kg} \cdot \text{m}^2} \right) \left(\frac{10 \text{ kpc}}{d} \right) \left(\frac{f}{100 \text{ Hz}} \right)^2 \left(\frac{\varepsilon}{10^{-6}} \right)$$

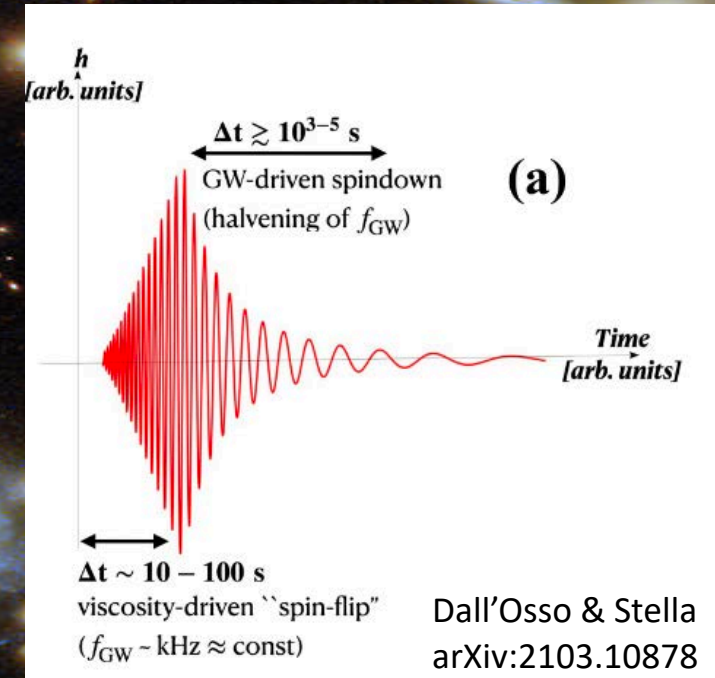
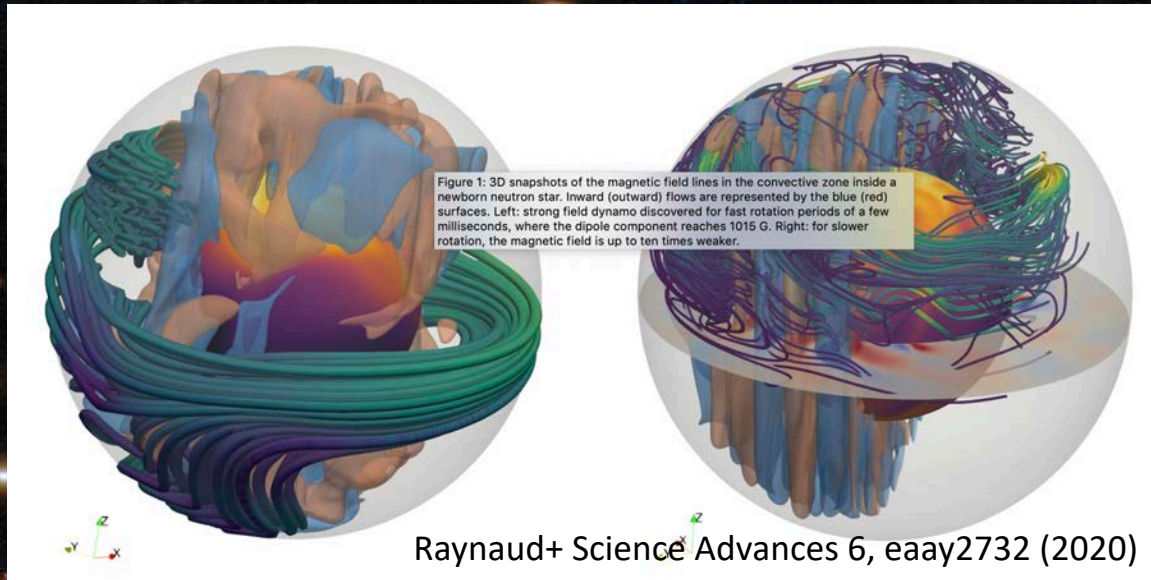
○ Expected signal maximum frequency below ~ 2 kHz.

○ The source we are searching for are in the Galaxy, $d < O(10 \text{ kpc})$

○ The ellipticity is largely unknown; $\varepsilon_{\text{max}} \sim 10^{-6}$ for standard NSs, but some exotic EOS foresee $\varepsilon_{\text{max}} \sim 10^{-4}$ or even more.

○ **What are the typical values?**

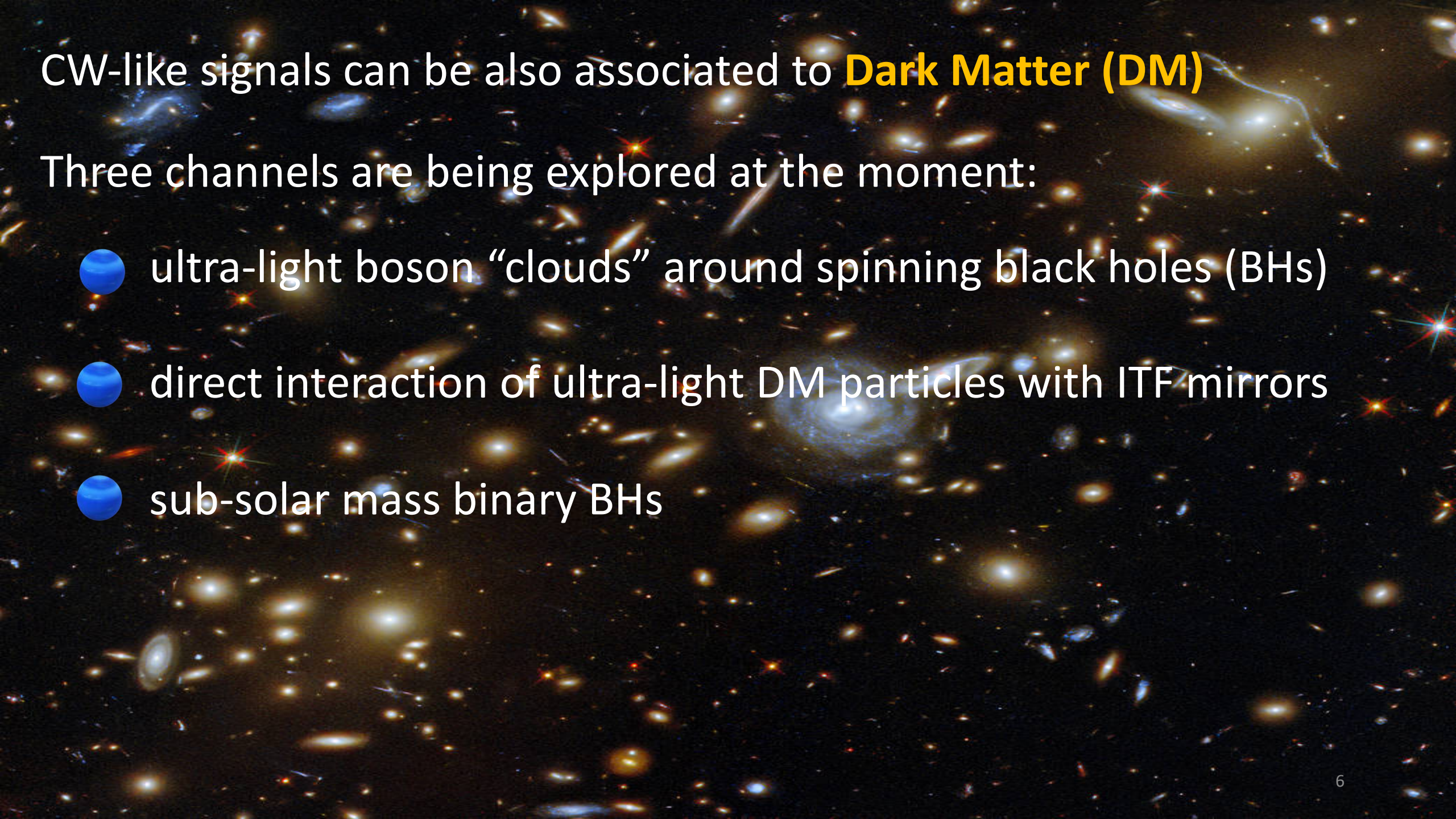
CW-like signals are also expected from newborn highly deformed neutron stars, like magnetars



The very strong spin-down makes these signals last hours-days in the detector sensitivity band

$$\epsilon_B = k (E_{B,\phi}/W) \approx 4 \times 10^{-4} (k/4) B_{\text{int},16}^2 R_6^4 M_{1.4}^{-2} \quad \text{ellipticity} \sim B^2$$

Magnetars formed in core collapse supernovae have an estimated event rate of 1 per year within ~ 10 Mpc



CW-like signals can be also associated to **Dark Matter (DM)**

Three channels are being explored at the moment:

- ultra-light boson “clouds” around spinning black holes (BHs)
- direct interaction of ultra-light DM particles with ITF mirrors
- sub-solar mass binary BHs

Ultra-light boson “clouds” should form around spinning BHs through superradiance, and then dissipate through GW emission [Arvanitaki+, PRD91, 084011 (2015)]

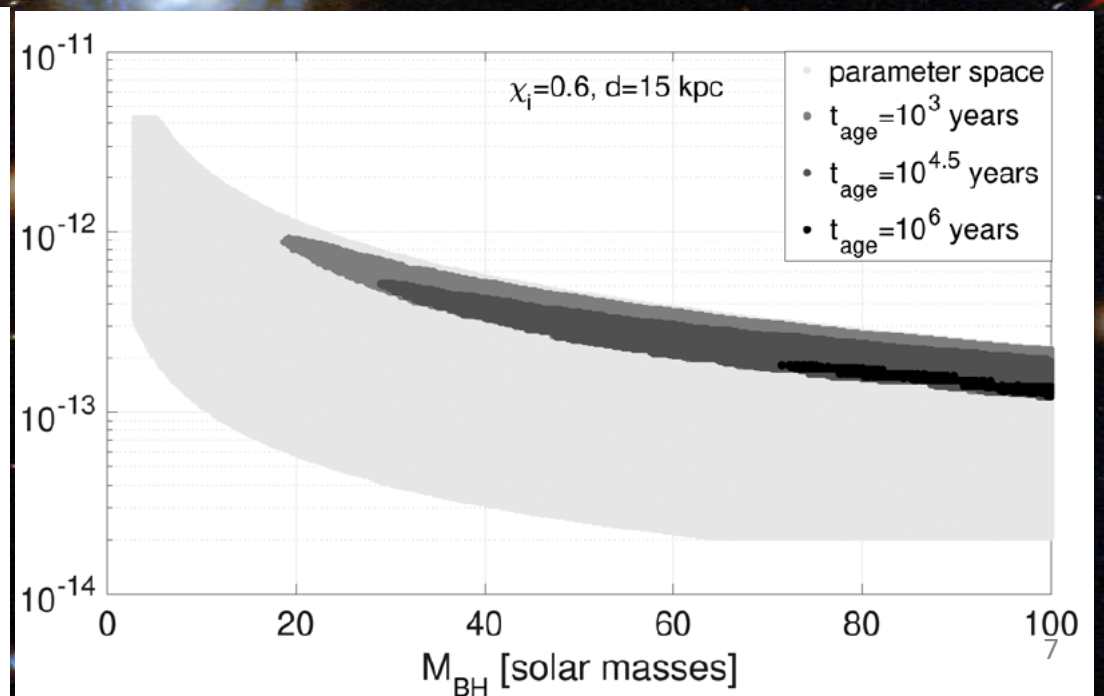
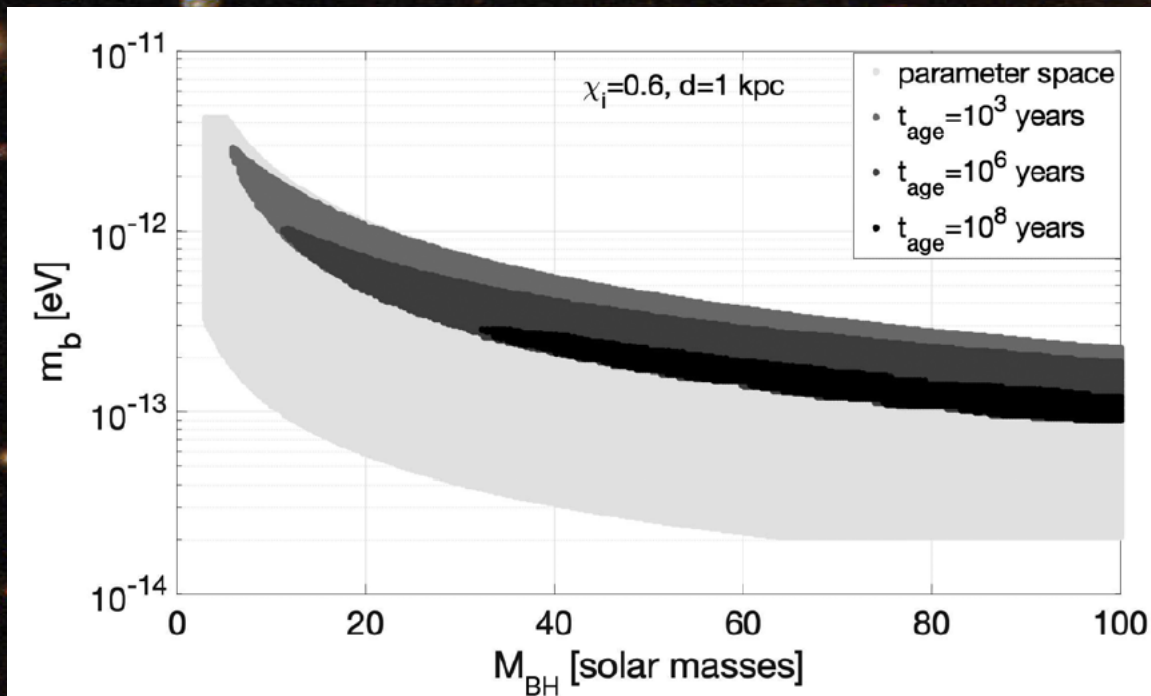
Signal mainly depends on the boson and BH mass

$$\frac{f_{\text{gw}}}{1 \text{ Hz}} \simeq 483 \left(\frac{m_b}{10^{-12} \text{ eV}} \right)$$

$$h_0 \approx 8 \times 10^{-28} \left(\frac{M}{10 M_\odot} \right) \left(\frac{\alpha}{0.1} \right)^7 \left(\frac{\text{Mpc}}{r} \right) \left(\frac{\chi - \chi_f}{0.1} \right)$$

$$\alpha = \frac{GM_{\text{BH}} m_b}{c \hbar}$$

Constraints on boson mass from a CW search in O2 data [Palomba+, PRL123, 171101 (2019)]



DM ultra-light candidates could directly interact with ITF components through different mechanisms

E.g. dark photons (DP) could couple to protons and/or neutrons of the mirrors producing a stochastic oscillatory force [Pierce+, PRD99, 075002 (2019)]

$$\langle h_{\text{total}}^2 \rangle = \langle h_D^2 \rangle + \langle h_C^2 \rangle$$

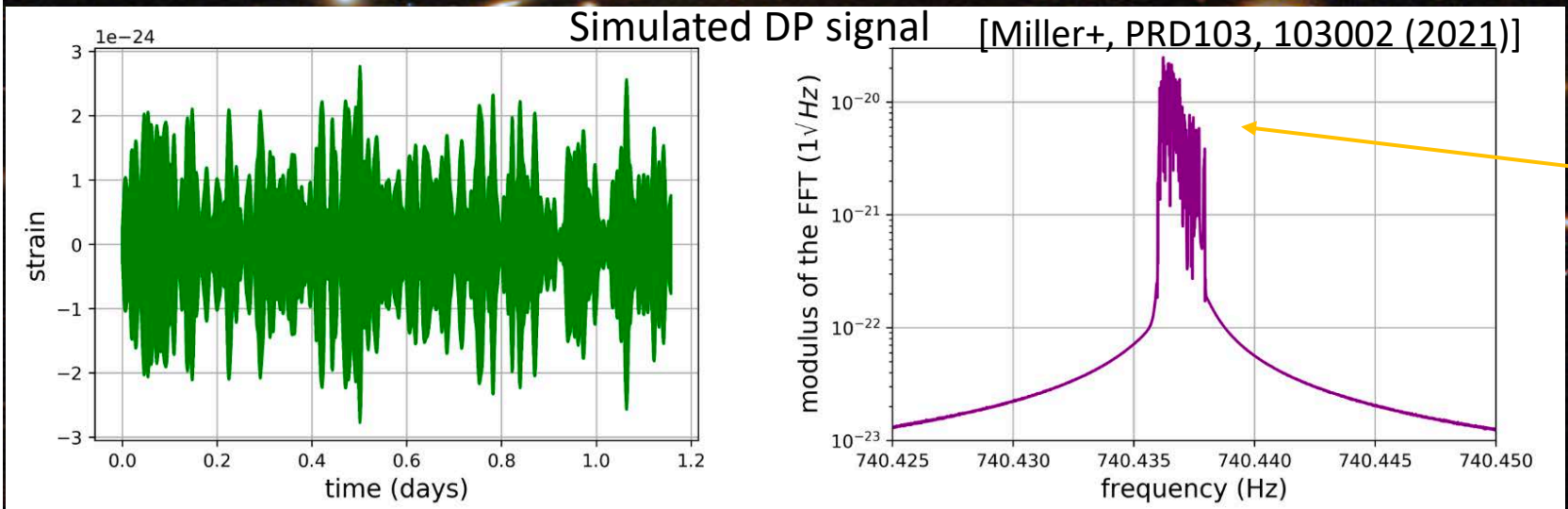
DP mass

$$f_0 = \frac{m_A c^2}{2\pi\hbar}$$

$$\sqrt{\langle h_D^2 \rangle} \simeq 6.56 \times 10^{-27} \left(\frac{\epsilon}{10^{-23}} \right) \left(\frac{100 \text{ Hz}}{f_0} \right)$$

ϵ : particle/DP coupling constant (normalized to EM coupling constant)

$$\sqrt{\langle h_C^2 \rangle} \simeq 6.58 \times 10^{-26} \left(\frac{\epsilon}{10^{-23}} \right)$$



Frequency spread related to the Maxwell-Boltzman velocity distribution of DPs

Searches for CWs

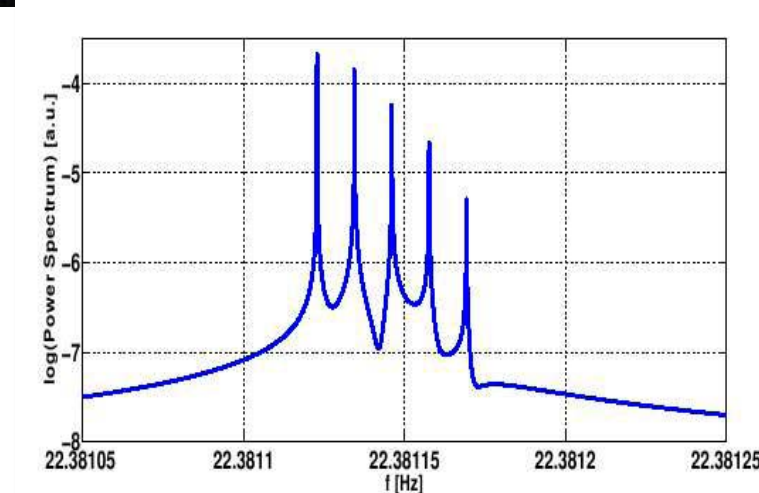
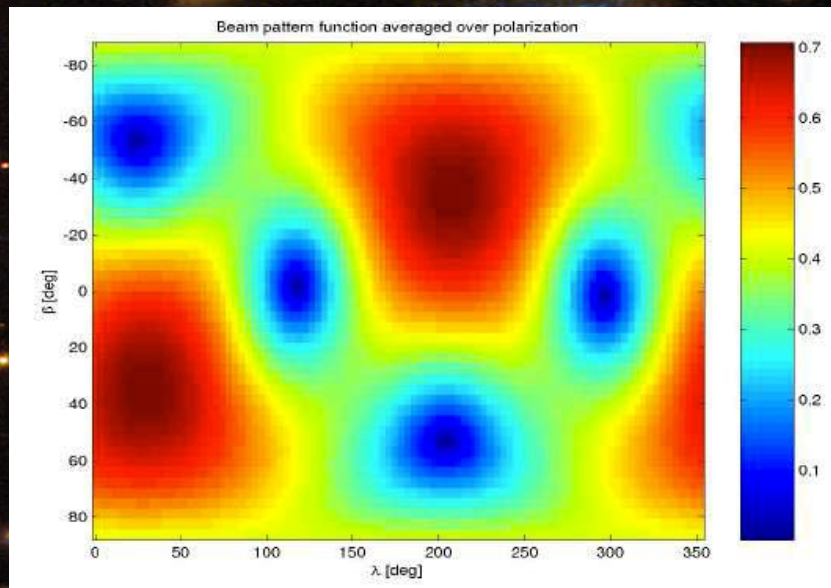
● Intrinsic signal frequency changes due to spin-down (up)

$$f_0(t) = f_0 + \dot{f}_0(t - t_0) + \frac{\ddot{f}_0}{2}(t - t_0)^2 + \dots$$

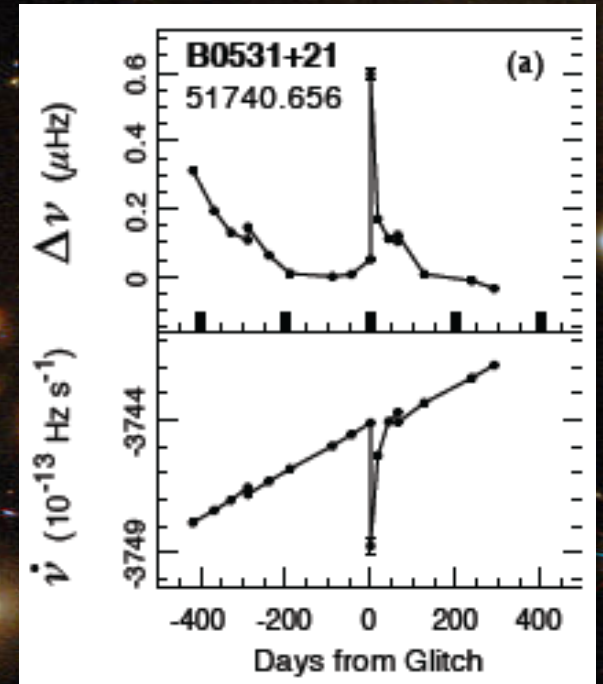
● Received signal frequency is affected by Doppler modulation (with a further modulation if the source is in a binary system)

$$f(t) = \frac{1}{2\pi} \frac{d\Phi(t)}{dt} = f_0(t) \left(1 + \frac{\vec{v} \cdot \hat{n}}{c} \right), \quad \vec{v} = \vec{v}_{orb} + \vec{v}_{rot}$$

● There is a sidereal phase and amplitude modulation due to the detector non-uniform response function



- Small relativistic effects (namely, Einstein and Shapiro delay) may play a role
- Pulsar glitches are likely to produce GW signal phase discontinuities
- Signal frequency random fluctuations can also be present

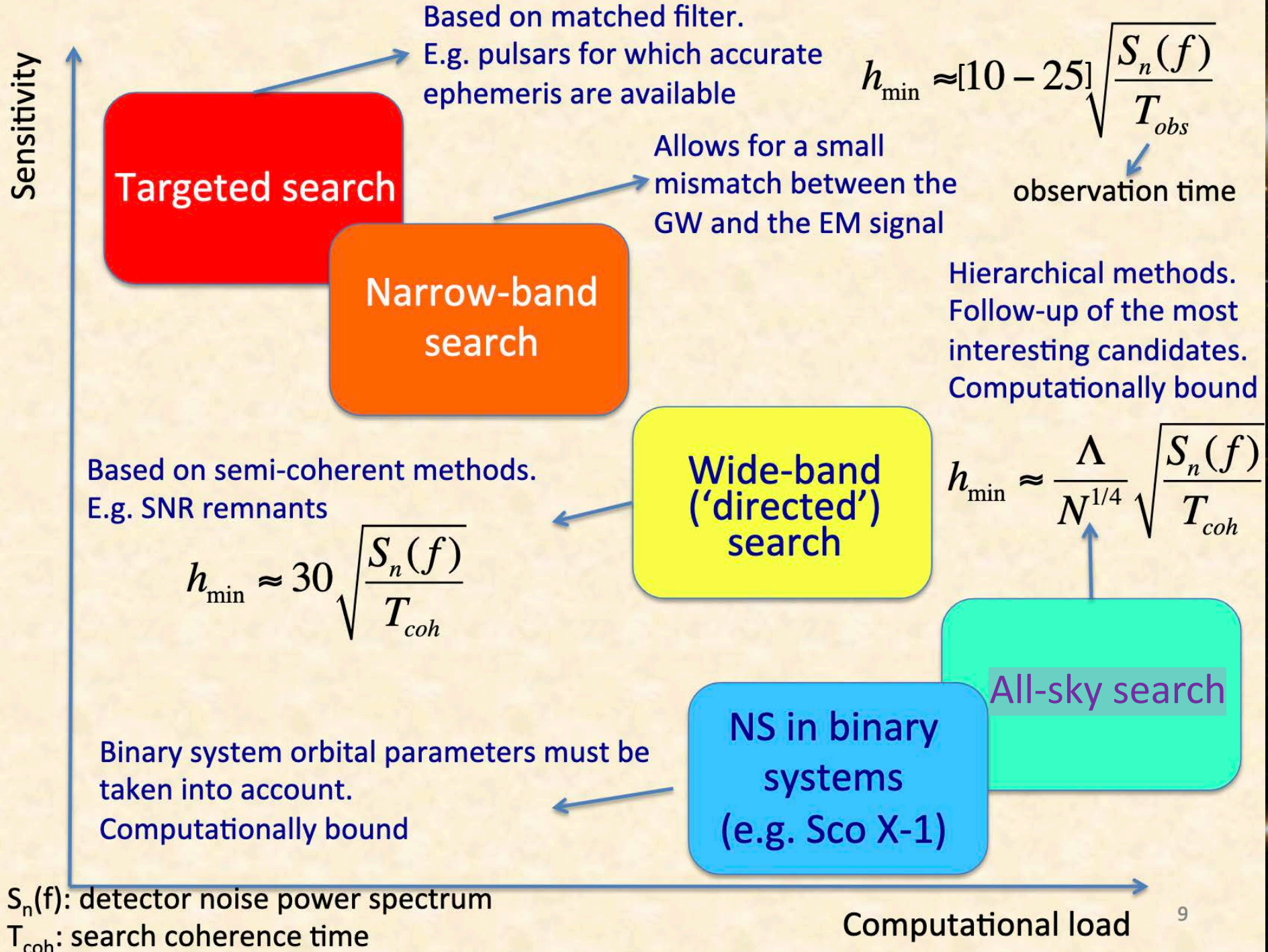


In general, signals are expected to be deeply buried into the noise

BUT

- signal duration very long respect to typical observation times → Signal-to-noise ratio increases with time
- signals have very specific time-frequency behavior → This helps also in rejecting noise artifacts

Robustness with respect to un-modeled signal features and noise artifacts would be the third leg in this plot



Some recent search results

- Based on O3 data (several analyses still on-going)
- See e.g. Sieniavska & Beijger, Universe 2019, 5, 217; doi:10.3390/universe5110217 for a (relatively) recent review of methods and past results

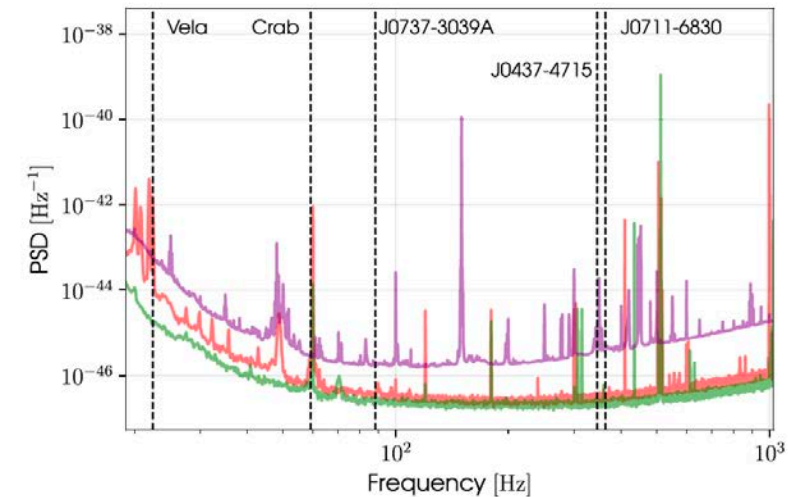


Figure 1. O3a noise PSD for H1, L1, and V1 shown in red, green, and purple. The H1 and L1 PSDs are calculated during a time period of optimal performance for the detector, while the Virgo PSD is averaged over the run. The vertical dashed lines indicate the searched frequency region for each of the five pulsars.

GWs constraints on the equatorial ellipticity of millisecond pulsars

Targets: 5 radio pulsars, O3a data

For the first time, a constraint on the fraction of spin-down energy due to GWs emission has been obtained for a millisecond pulsar

ApJL 902 L21, 2020

O3a covers April 1st –October 1st 2019

Full O3 targeted and narrow-band searches on-going

Pulsar name (J2000)	h_0^{sd} (10^{-26})	Analysis method	$C_{21}^{95\%}$ (10^{-26})	$C_{22}^{95\%}$ (10^{-27})	$h_0^{95\%}$ (10^{-26})	$Q_{22}^{95\%}$ (10^{32} kg m ²)	$\epsilon^{95\%}$	$h_0^{95\%}/h_0^{\text{sd}}$
Young pulsars ^a								
J0534+2200 ^b (Crab)	140	Bayesian	12.7(7.9)	6.3(5.6)	1.5(1.2)	6.6(5.7)	$8.6(7.4) \times 10^{-6}$	0.010(0.009)
		\mathcal{F}/\mathcal{G} -statistic	8.9(6.2)	7.9(7.1)	1.9(1.5)	7.9(6.3)	$10(8.1) \times 10^{-6}$	0.014(0.011)
		5n-vector	15.9(12.4)	...	3.0(2.9)	12.6(12.1)	$16.3(15.7) \times 10^{-6}$	0.021(0.021)
J0835–4510 (Vela)	330	Bayesian	1100(980)	120(84)	22(17)	91(73)	$12.0(9.5) \times 10^{-5}$	0.067(0.052)
		\mathcal{F}/\mathcal{G} -statistic	1470(1370)	116(48)	23(12)	96(50)	$12.4(6.4) \times 10^{-5}$	0.070(0.036)
		5n-vector	1700(1400)	...	24(24)	100(102)	$13.0(13.2) \times 10^{-5}$	0.073(0.073)
Recycled pulsars								
J0437–4715	0.79	Bayesian	2.2	4.1	0.78	0.0074	9.5×10^{-9}	0.99
		\mathcal{F}/\mathcal{G} -statistic	2.1	7.2	0.86	0.0082	11.0×10^{-9}	1.1
		5n-vector
J0711–6830	1.2	Bayesian	2.6	3.5	0.82	0.0064	8.3×10^{-9}	0.68
		\mathcal{F}/\mathcal{G} -statistic	2.4	9.4	0.98	0.0059	7.7×10^{-9}	0.82
		5n-vector	2.9	...	0.91	0.0053	7.2×10^{-9}	0.76
J0737–3039A	0.62	Bayesian	5.9	3.3	0.69	0.80	1.0×10^{-6}	1.1
		\mathcal{F}/\mathcal{G} -statistic	3.0	1.2	0.99	1.10	1.4×10^{-6}	1.6
		5n-vector

All-sky search for CWs from unknown NSs in binary systems

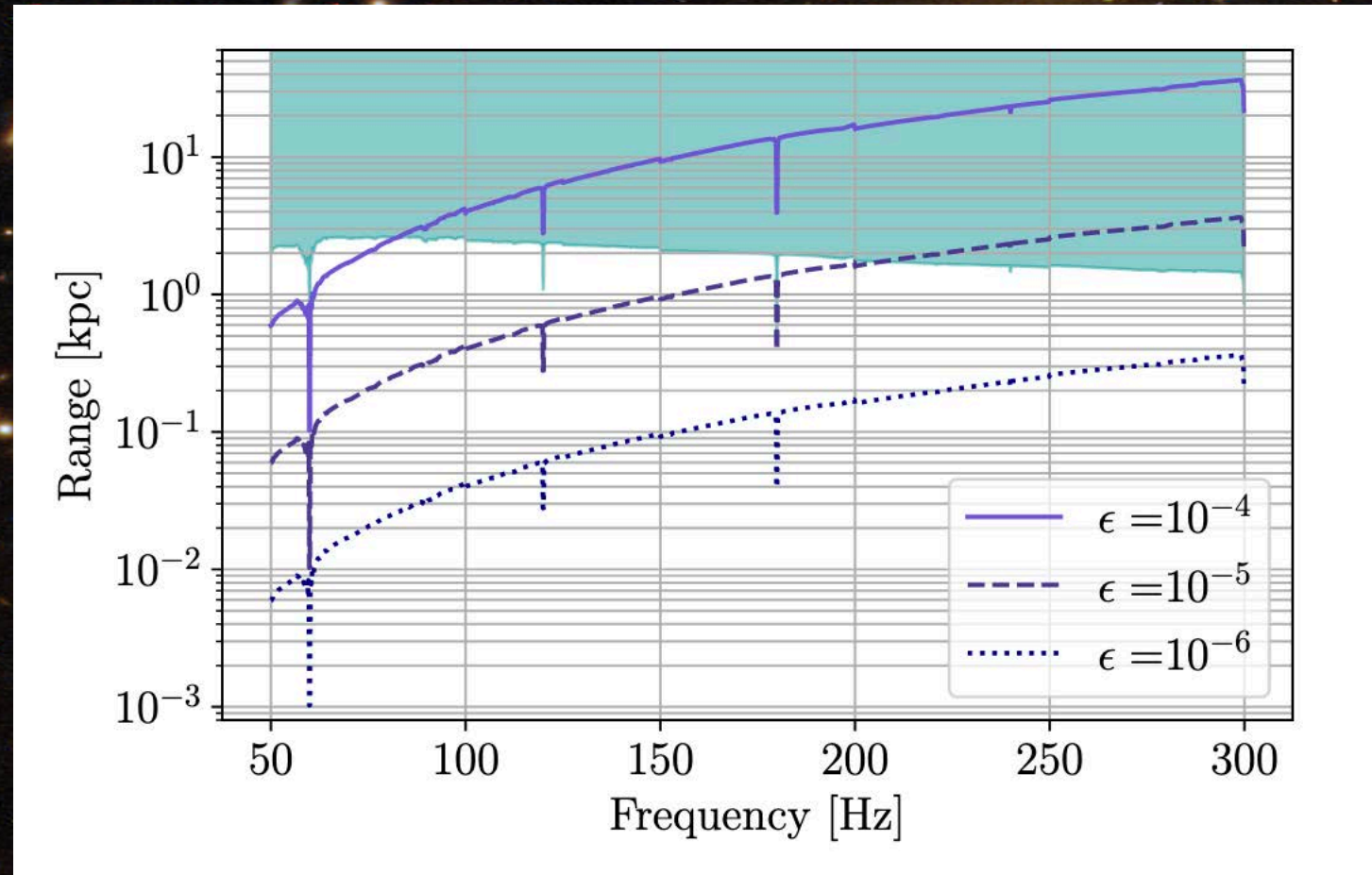
PRD 103 064017, 2021

O3a data

Frequency range: [50, 300] Hz

Orbital period range of [3, 45] days and projected semi-major axis of [2, 40] l-s

GPU-accelerated pipeline



Constraints from the energetic young X-ray pulsar PSR J0537-6910

ApJL 913 L27, 2021

PSR 0537-6910 is also known as the “big glitcher”

Ephemerides from NICER data

Full O3 LIGO/Virgo data

Search at both once and twice $f_{\text{rot}}=62$ Hz

For the first time for this pulsar, we have been able to constrain the fraction of spin-down energy due to GW (less than 14%)

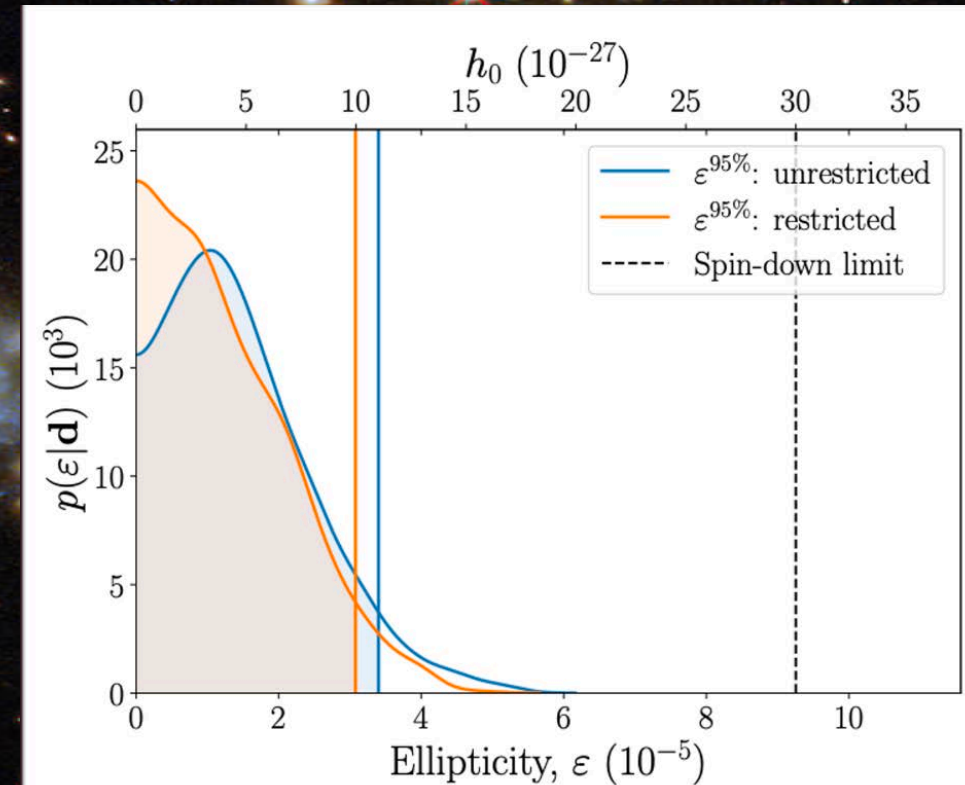


Figure 4. Posterior probability distribution for ellipticity and h_0 for the analyses with unrestricted and restricted priors on the pulsar orientation. The 95% credible upper limits are shown as vertical colored lines, while the spin-down limit is given by the vertical dashed black line. 15

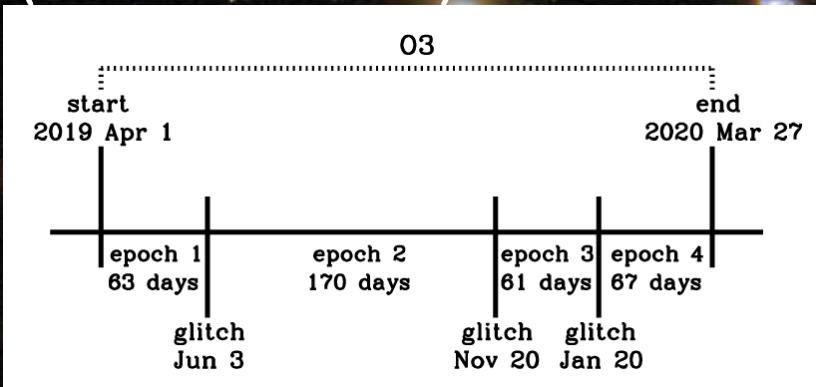
Constraints on GW emission due to r-modes in the glitching pulsar PSR J0537-6910

Accepted in ApJ
(2104.144170)

Full O3 search, motivated by the measured inter-glitch braking index which suggests that r-modes could be active

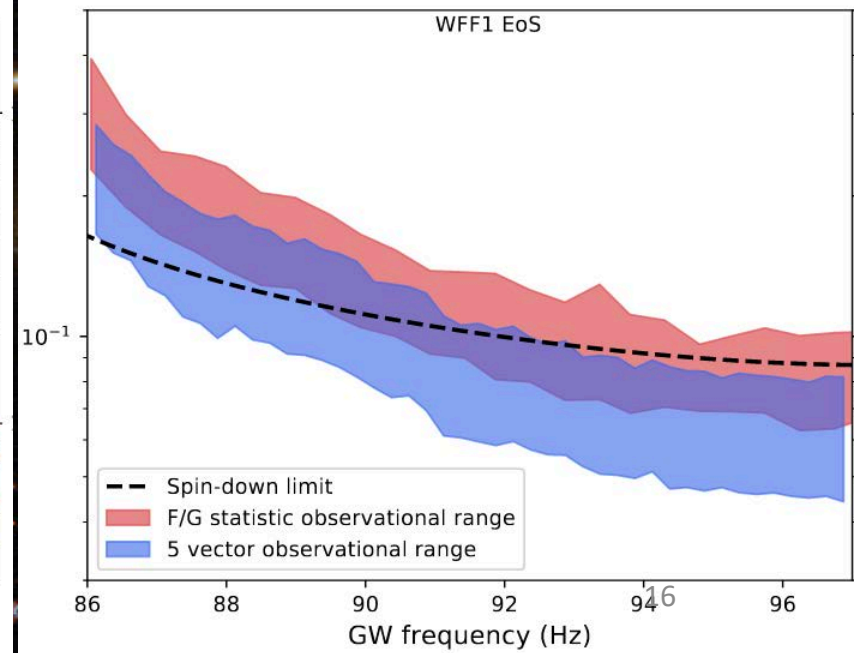
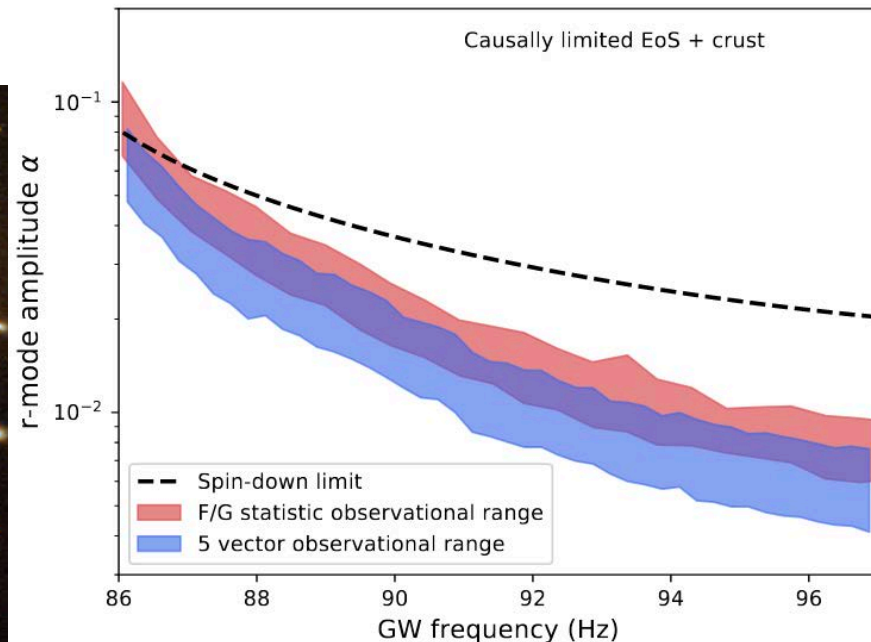
$$\alpha = \sqrt{\frac{5}{8\pi}} \frac{c^5}{G} \frac{h_0}{(2\pi f)^3} \frac{d}{MR^3 \tilde{J}}$$

$$\approx 0.017 \left(\frac{90 \text{ Hz}}{f}\right)^3 \left(\frac{h_0}{10^{-26}}\right)$$



Frequency range:
[86, 97] Hz to deal with
EOS uncertainty

Ephemeris obtained.
from NICER data



CW search from young supernova remnants

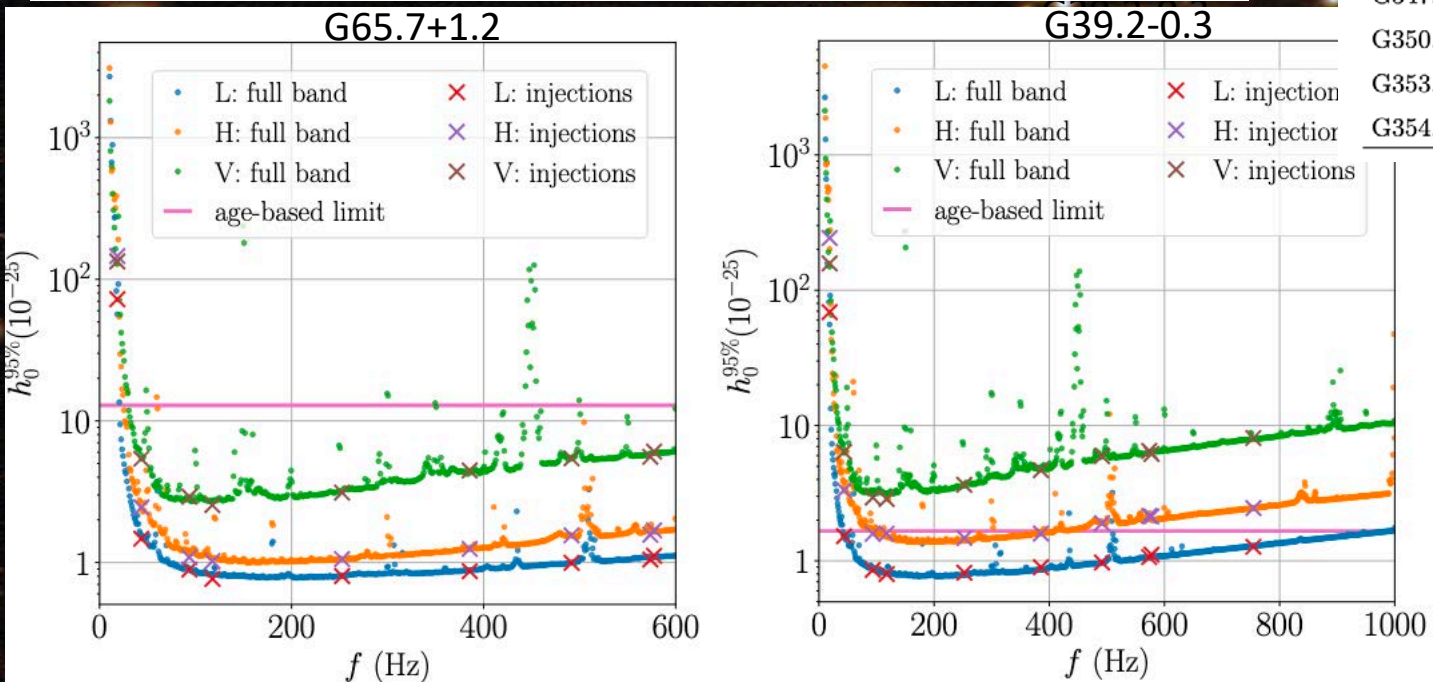
Submitted to ApJ (2105.11641)

15 SNR, O3a data, 3 algorithms

Frequency range: [10, 2000] Hz

$$h_0^{\text{age}} = 2.27 \times 10^{-24} \left(\frac{1 \text{ kpc}}{D} \right) \left(\frac{1 \text{ kyr}}{t_{\text{age}}} \right)^{1/2} \left(\frac{I_{zz}}{10^{38} \text{ kg m}^2} \right)^{1/2}$$

Source	Minimum t_{age} (kyr)	D (kpc)	T_{coh} (hours)	f (Hz)	\dot{f} (Hz/s)
G1.9+0.3	0.10	8.5	1.0	[31.56, 121.7]	$[-3.858 \times 10^{-8}, 3.858 \times 10^{-8}]$
G15.9+0.2	0.54	8.5	1.0	[44.03, 657.1]	$[-3.858 \times 10^{-8}, 3.858 \times 10^{-8}]$
G18.9-1.1	4.4	2	1.9	[31.02, 1511]	$[-1.507 \times 10^{-8}, 1.507 \times 10^{-8}]$
G39.2-0.3	3.0	6.2	2.8	[62.02, 459.2]	$[-1.968 \times 10^{-8}, 1.968 \times 10^{-8}]$
G65.7+1.2	20	1.5	4.7	[35.10, 1128]	$[-3.149 \times 10^{-9}, 3.149 \times 10^{-9}]$
G93.3+6.9	5.0	1.7	1.9	[30.00, 1668]	$[-1.335 \times 10^{-8}, 1.335 \times 10^{-8}]$
G111.7-2.1	0.30	3.3	1.0	[25.71, 365.1]	$[-3.858 \times 10^{-8}, 3.858 \times 10^{-8}]$
G189.1+3.0	3.0	1.5	1.4	[26.13, 2000]	$[-1.968 \times 10^{-8}, 1.968 \times 10^{-8}]$
G266.2-1.2	0.69	0.2	1.0	[18.36, 839.6]	$[-3.858 \times 10^{-8}, 3.858 \times 10^{-8}]$
G291.0-0.1	1.2	3.5	1.0	[31.97, 1460]	$[-3.858 \times 10^{-8}, 3.858 \times 10^{-8}]$
G330.2+1.0	1.0	5	1.1	[36.57, 1039]	$[-3.858 \times 10^{-8}, 3.858 \times 10^{-8}]$
G347.3-0.5	1.6	0.9	1.0	[21.74, 1947]	$[-3.858 \times 10^{-8}, 3.858 \times 10^{-8}]$
G350.1-0.3	0.60	4.5	1.0	[31.96, 730.1]	$[-3.858 \times 10^{-8}, 3.858 \times 10^{-8}]$
G353.6-0.7	27	3.2	10	[77.86, 318.3]	$[-2.295 \times 10^{-9}, 2.295 \times 10^{-9}]$
G354.4+0.0	0.10	5	1.0	[25.72, 121.7]	$[-3.858 \times 10^{-8}, 3.858 \times 10^{-8}]$



$h_{0,\text{min}} \sim 7.7 \cdot 10^{-26}$ for G65.7+1.2

$\epsilon_{\text{min}} \sim 6 \cdot 10^{-8}$ for G266.2-1.2/Vela Jr.

Search sensitive to a possible spin wandering

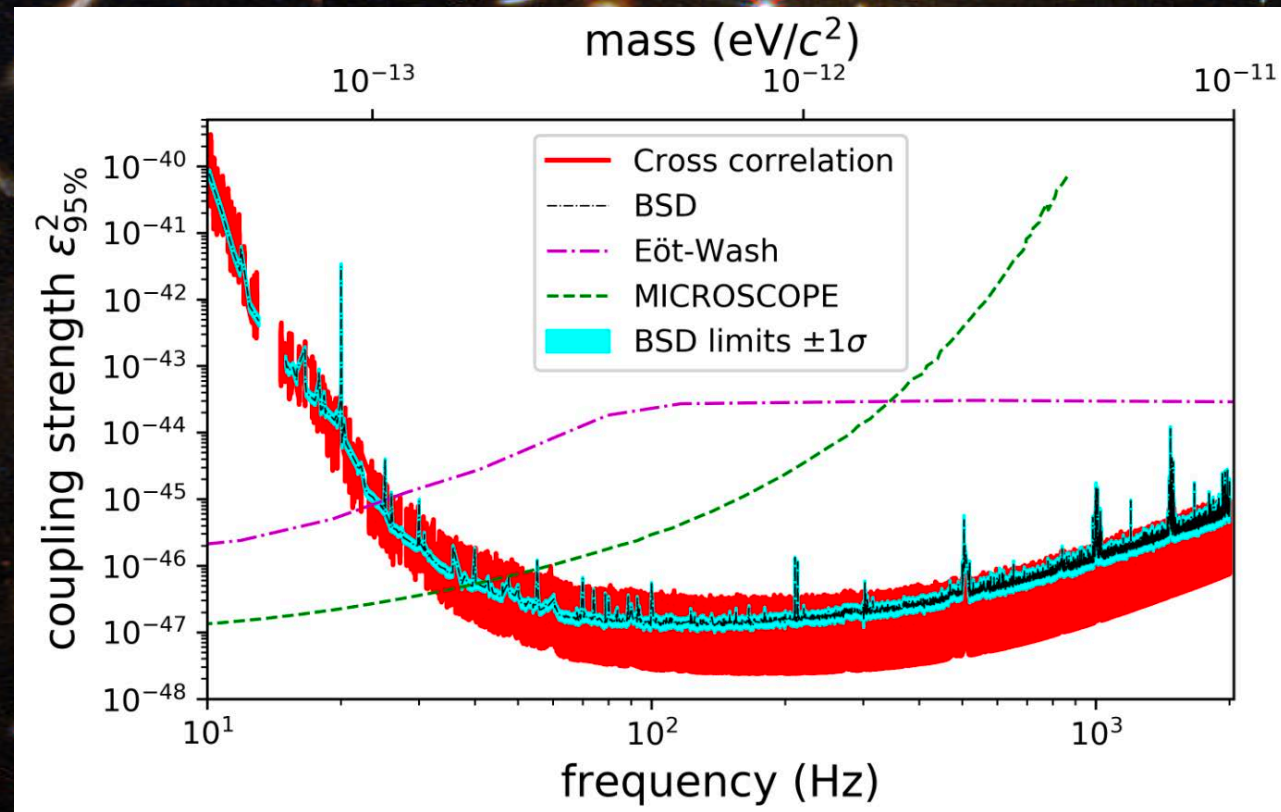
Constraints on dark photon dark matter using data from LIGO's and Virgo's third observing run

PRL, submitted (2105.1385)

Full O3 search, 2 pipelines

Explored DP mass range: $10^{-14} - 10^{-11}$
 eV/c^2

Improvement of $O(100)$ w.r.t. dark matter direct detection experiments in the range $[2 - 4] 10^{-13} \text{eV}/c^2$

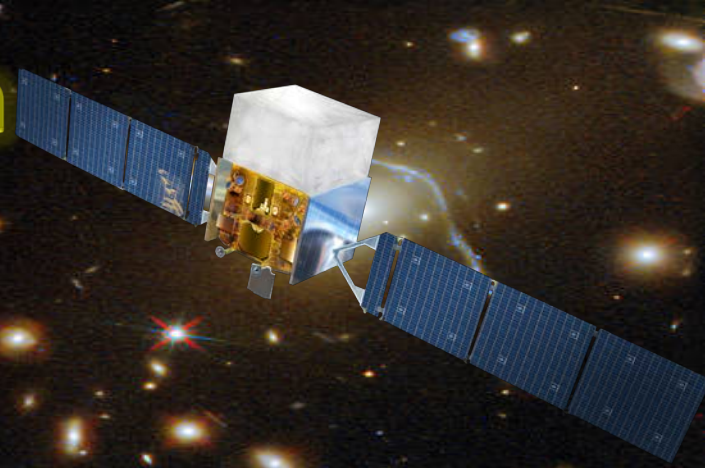


Multi-messenger approach

EM observations are crucial for:

- more sensitive searches of known sources
 - updated ephemeris
 - restricted parameter space
- searches of new potentially promising sources
- possible confirmation/identification of all-sky search candidates
- estimate distance to the source (which would allow to extract physical information from the measured strain)

The connection among GWs searches and DM will likely strengthen



Future prospects

We are currently completing O3 analyses

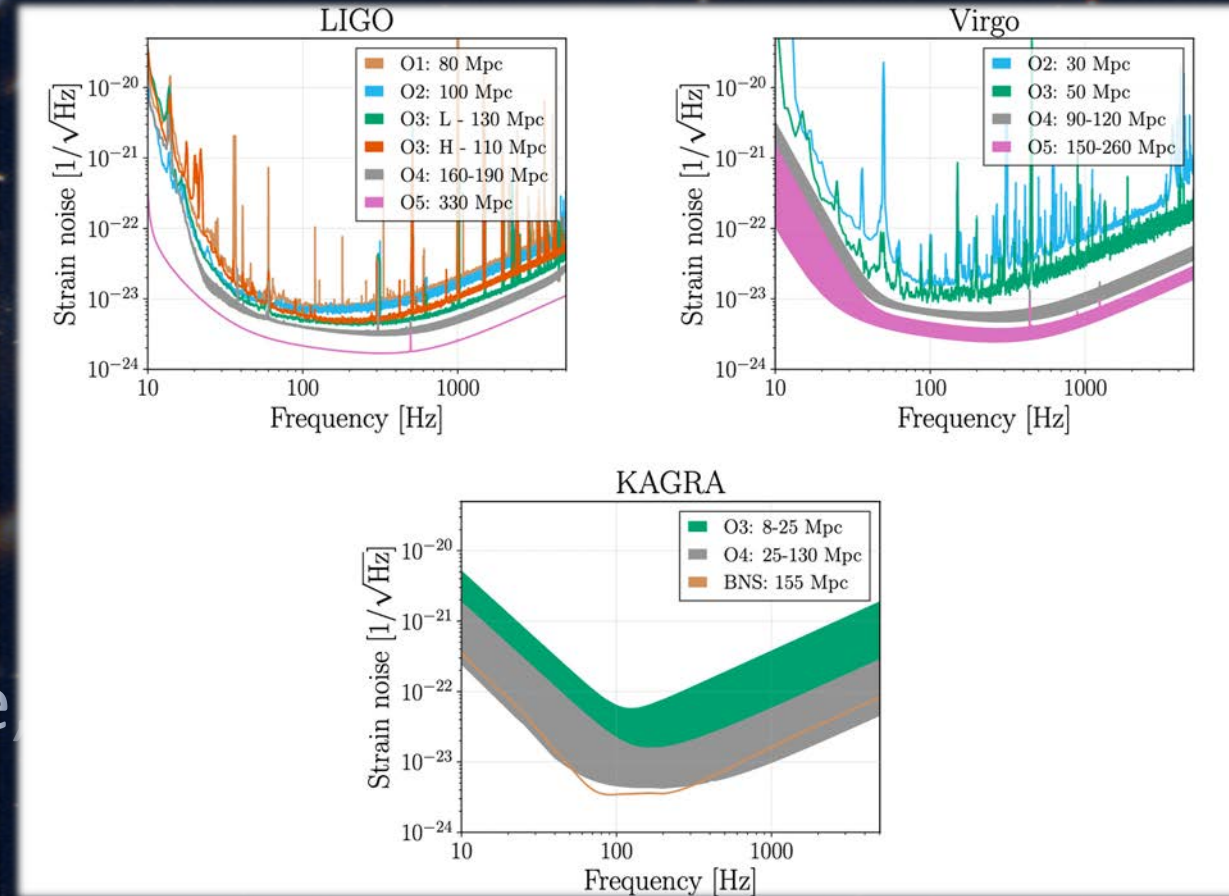
Three crucial ingredients to increase chance of detecting CWs are:

More sensitive, robust and fast searches

More sensitive detectors

2G → 2.5G → 3G (Einstein Telescope
Cosmic Explorer)

New sources



A deep-field astronomical image showing a dense population of galaxies. The galaxies are diverse in color, including bright yellow and orange, blue, and red. They vary in shape, from smooth, elliptical forms to more complex, irregular structures. The background is a deep black, punctuated by the light of these distant celestial bodies.

Thank you for the attention!